# Pore-scale Imaging of Oil-brine Movement During Waterflooding with Wettability Alteration from Tight Sandstone

**Cheng Liu***, **Yanjun Yin**, **Ruiting Bai**, CNOOC EnerTech-Drilling and Production Company, Tianjin, China; **Dengke Liu**, Xi'an Jiaotong University, Xi'an, China

## Abstract

To clarify the impact of salinity waterflooding on oil displacement efficiency and the microscopic mechanism, we have used micro-CT, nuclear magnetic resonance, high-pressure mercury injection, and other means to conduct an experimental analysis of salinity waterflooding. The results show that imbibition has little contribution to oil displacement efficiency, and the change in wettability is the main microscopic mechanism of low salinity waterflooding. However, the presence of corner flow can lead to a large amount of dropwise residual oil distribution, affecting the waterflooding effect, and seriously restricting oil recovery. When a strong hydrophilic phenomenon existed, pore size is no longer a key control factor for oil displacement efficiency. This study provides a theoretical reference for the influencing factors of different displacement methods on oil displacement efficiency.

## Introduction

The alteration of wettability is the most common reservoir property change in the secondary and tertiary oil recovery processes such as water flooding, chemical flooding and biological flooding (Sun et al. 2017; Druetta et al. 2019; Fani et al. 2022). Clarifying the change trend of wettability before and after water flooding can effectively predict water flooding efficiency. Previous studies believe that the increase of water wetness will significantly improve the oil displacement efficiency, while the understanding of the effect of the change of interface properties on oil recovery is different (Awolayo et al. 2016; Dordzie and Dejam 2021). Besides, to our knowledge, this conclusion is just an assumption and has not been rigorously manifested, nor has pore-scale direct analytical evidence supporting this finding. Meanwhile, capillary force is still dominant at the pore scale, wettability alteration due to clay migration may provide additional connectivity at some regions of the pore space, resulting in the evolution of fluid flow path and may improve the ultimate recovery rate (Rücker et al. 2015). Therefore, it is vital for the researchers to do some investigation on the pore-scale imaging of the waterflooding and the analysis of the relevant microscopic flow path change.

To test the conjecture, microscale spontaneous imbibition and waterflooding tests need to be done, and the resultant change in the pore network and wettability can be used to explain the fluid flow path evolution under different conditions. Techniques such as scanning electron microscopy (SEM) and microfluidic chips have been


DOI:10.14800/IOGR.1252
Received March 12, 2023; revised May 24, 2023; accepted June 28, 2023.
* Corresponding author: liucheng14@cnooc.com.cn

applied to observe this change (Sameni et al. 2015; Song and Kovscek 2015; Amirian et al. 2019). However, it is hard for SEM technique to provide the same field of view during spontaneous imbibition and waterflooding, and microfluidics lack real sandstones properties. The state-of-art X-ray micro-CT could provide images which has enable the brine and oil inside the pore space to be segmented at high resolution in the sandstones and shale (Mayo et al. 2015). Indeed, some studies have successfully imaged different kinds of fluid with the help of CT (Liu et al. 2017). Furthermore, the impact of wettability alteration on fluid flow evolution and concomitant wettability alteration have not hitherto been quantified directly at the pore scale.

Here, we design a new micro-CT image analysis workflow where we proposed a test protocol in which brine with different salinity are injected at varies degree of flooding rate during unsteady-state core imbibition-flooding experiments. We determine the wettability alteration after waterflooding with different brine salinity. Based on a workflow of spontaneous imbibition and waterflooding processes, the influencing factors of wettability alteration were investigated. Moreover, the underlying mechanisms of wettability alteration at pore-scale were analyzed.

## Methodology

**Materials.** We used a tight sandstone sample from C7 Formation in Ordos Basin, China. The sample was first cleaned to remove the oil by a mixture of ethanol and benzene (3:1), then it was dried at atmospheric pressure and 60 ℃ temperature. Before the CT scanning, a contact angle measurement was performed in the original rock to determine the wettability. The fluid mixed with deionized water and 2.5 wt% NaI was used as the brine to increase the reflection signal. Different concentrations of brine (sodium chloride, NaCl) functioned as the aqueous phases. The crude oil was selected from Ordos Basin in China, then mixed with aviation kerosene (20 wt%) to make its viscosity meet the in-situ situations in the reservoirs. Apart from aviation kerosene, 20 wt% iododecane was added to improve X-ray contrast. Hence, two types of fluids were used during the tests: brine with different salinity and doped-oil.

**Experimental Procedures**. The imbibition and waterflooding test were conducted in a Hassler type flow cell manufactured by Vinci Technologies, and the cell was made of carbon fiber epoxy to pre-serve the X-ray signal (Lebedev et al. 2017). Zeiss Xradia 610 Versa micro-CT instrument was used for high-resolution imaging, with 85 keV energy, 5.305 μm voxel size, 2s exposure time for each slice, and 518 projections with 513×515×370 voxels. The detailed experimental processes with different conditions are as follows:

1. Dry condition: Place the specimen inside the cell, and vacuum the system. After 6 h, a CT scan was performed.
2. Saturation condition: The specimen was saturated with high-salinity brine, and the fluid flow rate was 1 ml/min. When the pressure between the inlet and outlet were remain the same, turned down the pump and conducted CT scanning for the specimen.
3. Drainage condition: Set the flow rate at 0.01 ml/min, and injected the mixed crude oil into the specimen. Like the above step, a CT scan was performed when the differential pressure was inexistent.
4. Spontaneous imbibition condition: Set the flow rate at 0.01 ml/min, and injected the high salinity brine into the specimen. The apparent brine permeability was calculated by the data from inlet and outlet pressure. When the differential pressure vanished, we acquired the image.
5. High salinity brine waterflooding condition: Flow the low salinity brine at 0.5 ml/min, and measured the differential pressure to determine the end time. The apparent permeability was calculated and the image was captured.
6. Low salinity brine waterflooding condition: Performed the low salinity brine water-flood with an injection rate of 0.5 ml/min, measured the apparent permeability, and took an image. After this step, another brine with lower salinity was injected into the specimens, and those mentioned parameters were also determined.

**Figure 1** demonstrates the workflow of the experiments.

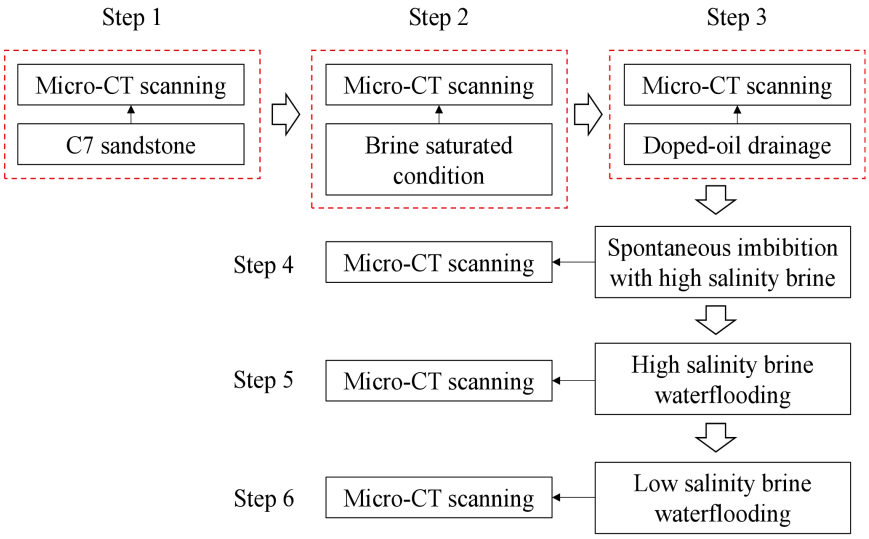


**Figure 1—Flowchart to demonstrate the experimental processes.**

## Results

**Phases Behavior before Spontaneous Imbibition**. As seen in **Figure 2**, the greyscale value for vacuumed pores was much lower than the value for minerals, and the first one nearly remains the same, while the latter one has a range of distribution, indicating different kinds of minerals, such as detrital grains and clay. Clay minerals are loosely distributed in pore spaces; therefore, the relatively dark areas (low greyscale value) in the pores or encircle the grains are identified as clays (Aksu et al. 2015; Kamal et al. 2019). After saturation, almost all pores are filled with brine, indicating that the overall connectivity of the sample is strong (Figure 2b). After drainage, the fluid in a single pore is almost single-phase, such as full of brine or crude oil, just a small number of single pores coexist with two kinds of fluids (Figure 2c). It is worth noting that the pores enriched by clay minerals are almost full of oil phase after drainage. Since clay minerals are usually hydrophilic (Kooli et al. 2014), it also proves that the sample has good overall connectivity.

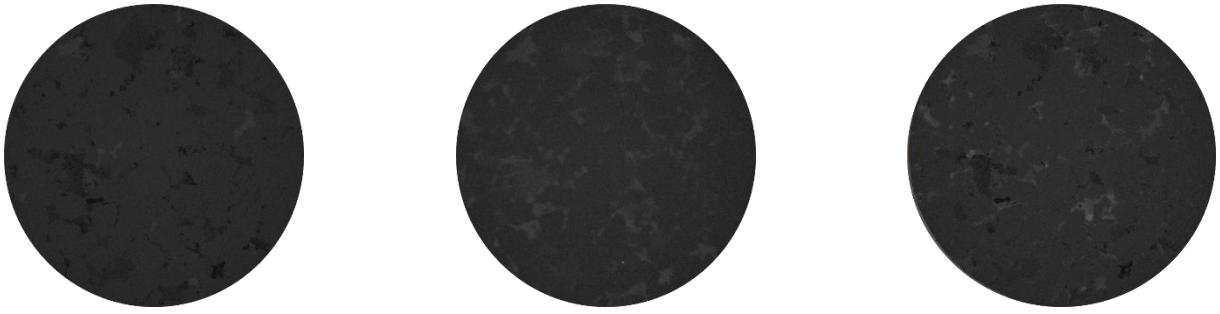

(a) Dry sample (b) After brine saturation (c) After drainage

**Figure 2—Grayscale and phase-segmented CT images for 2D slices during different steps before spontaneous imbibition.**

**Phases Behavior after Spontaneous Imbibition and Waterflooding**. **Figure 3** shows the distribution of oil and brine after spontaneous imbibition. Spontaneous imbibition has little impact on the overall recovery (Figure 3). It can only be seen that the integral rate of brine phase in some small holes increases, indicating that spontaneous imbibition in hydrophilic rocks mainly improves recovery by thickening the water film. However, because the core is relatively dense and the connectivity is relatively poor, the overall effect on improving recovery is small.

(a) After spontaneous imbibition

(b) After high salinity brine waterflooding

(c) After low salinity brine waterflooding

**Figure 3—Grayscale and phase-segmented CT images for 2D slices during different steps after spontaneous imbibition and waterflooding.**

**Figure Segmentation.** According to the helium porosity data, the gray value division interval is determined, and then the proportion of pores brines, and oil in different stages is obtained by image segmentation. **Figure 4a-c** represents the phase-segmented CT images for dry, after saturation, and after drainage conditions, respectively.

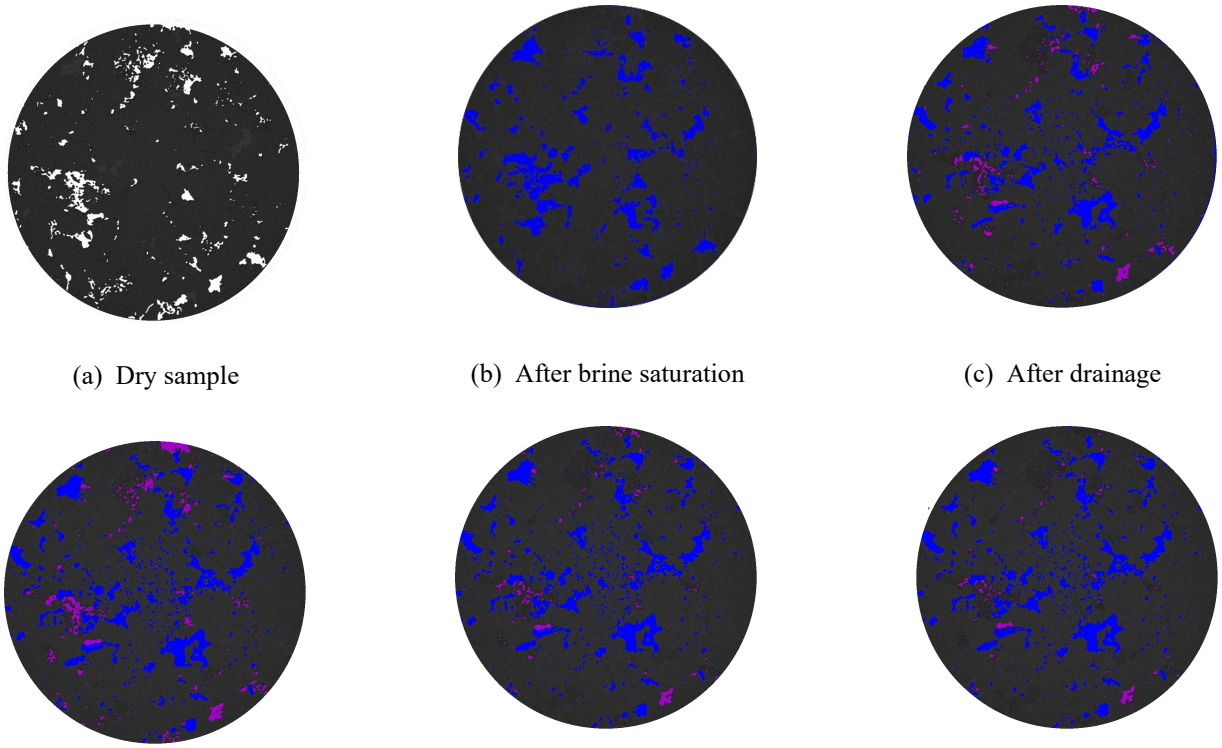

(a) Dry sample

(b) After brine saturation

(c) After drainage

(d) After spontaneous imbibition

(e) after high salinity brine waterflooding

(f) After low salinity brine waterflooding

**Figure 4—The segmented phase volume fractions of different stages in each slice: from the inlet 0 to the end (White, blue, and pink represent pores, brine, and oil, respectively).**

## Discussion

Due to the complex pore structure of rock samples, the influence of gravity on oil dis-placement efficiency can be almost ignored in the spontaneous imbibition stage, so the difference in wettability directly causes the difference in

oil displacement efficiency (Xu et al. 2019). The CT results of four samples show the degree of hydrophilicity of rock samples and the oil displacement efficiency at the spontaneous imbibition and waterflooding stages.

**The Impact of Wettability Alteration on Waterflooding Mode.** The existence of corner flow is the main reason for the waterflooding mode alteration (Watson and Weinstein 1971). As shown in Figure 5, the clastic particles of the rock samples in the study area are mainly sub-angular and sub-rounded, with roundness generally less than 0.8 (Krumbein calculation method) (Krumbein 1941), which has the formation conditions of corner flow. The average round-ness of the four samples is between 0.6-0.8, so the two-dimensional model of a pore channel can be equivalent to a plane with an angle of 100 ° (90 ° is completely corner, 180 ° is completely spherical).

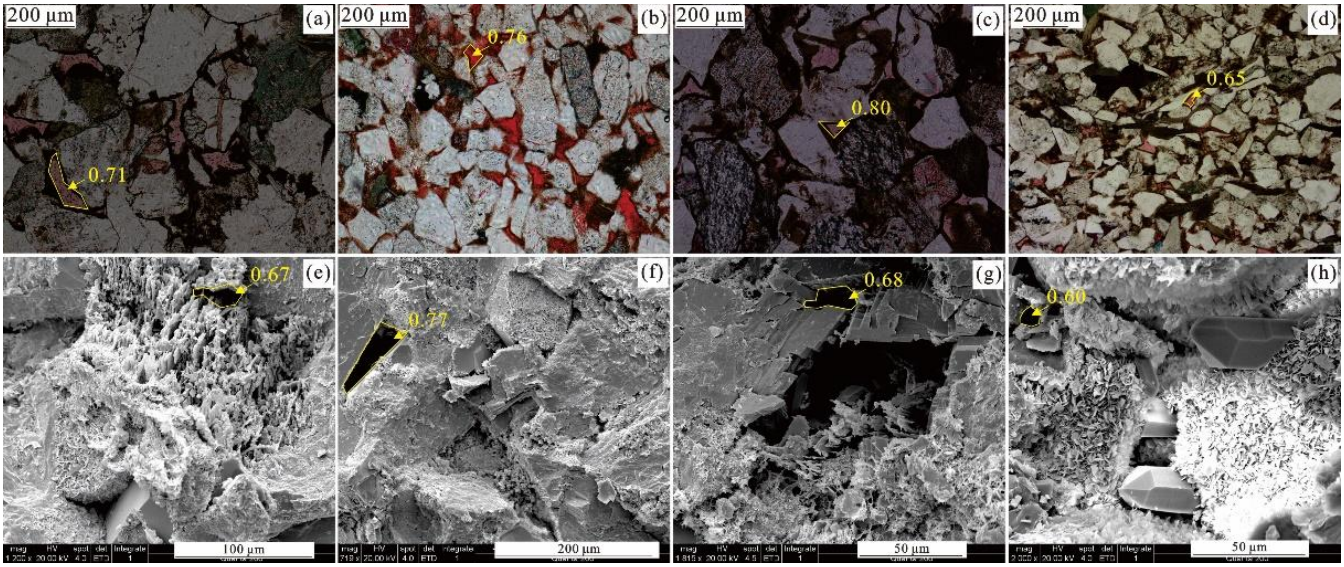


**Figure 5—Casting thin sections and SEM images in the research area. The numbers represent the roundness of the circled pores. (a), (e) Sample 1. (b), (f) Sample 2. (c), (g) Sample 3. (d), (h) Sample 4.**

As shown in **Figure 6**, under the condition of spontaneous imbibition stages, the penetration rate of the front end of corner flow is related to the particle-particle angle and the degree of hydrophilic: the smaller the angle, the higher the degree of hydrophilic, the higher the penetration rate. When the contact angle is less than 50 °, due to the existence of corner flow, the water film will advance in a completely spontaneous imbibition mode, which will lead to the displacement velocity at the edge of the channel is far greater than that at the center of the hole, resulting in the continuous formation of oil in water, and the single hole oil displacement efficiency is reduced. Although the swept area is increased, the overall recovery factor is low. When the contact angle is greater than 50 °, the corner flow cannot be formed, and the water film steadily advances the front end of the water drive in a semi-arc shape. The overall oil displacement efficiency is high, so the recovery factor is high. This result shows that reducing wettability too much will lead to a large amount of corner flow, and a large amount of filamentous residual oil will be formed in the reservoir, which only increases the swept area and seriously restricts the single-hole oil displacement efficiency and a negative impact on oil recovery.

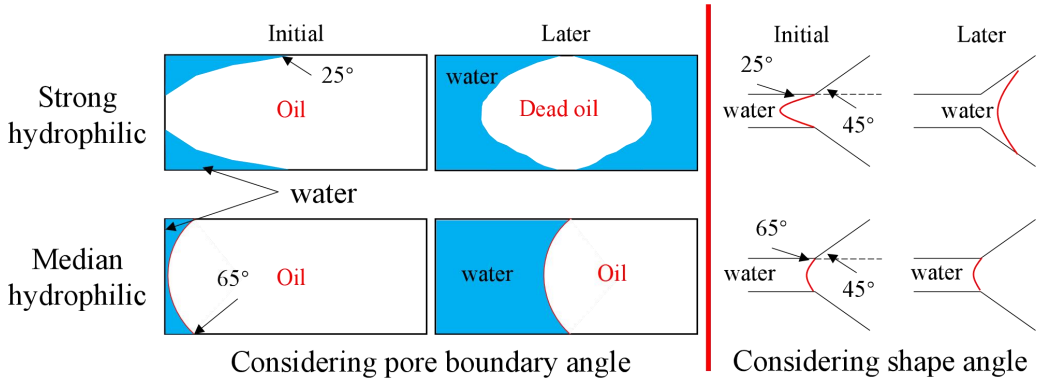


**Figure 6—Fluid movement behavior concerning corner flow and pore-throat-shaped angle**

**Waterflooding Recovery Trend Evolution.** The recovery rate at different stages also shows an interesting trend (**Figure 7**). Although the spontaneous imbibition oil displacement efficiency of sample 1 is the highest, the improvement in the subsequent waterflooding stage is not obvious. This trend means that the starting pressure of dropwise residual oil is far greater than that of flaky residual oil, and a large amount of residual oil caused by water film penetration in the early stage is difficult to produce even if the viscosity displacement is increased. Therefore, we should not pursue imbibition development excessively for reservoirs with high hydrophilic, and we need to configure relatively high displacement power to maximize the efficiency of reservoir development.

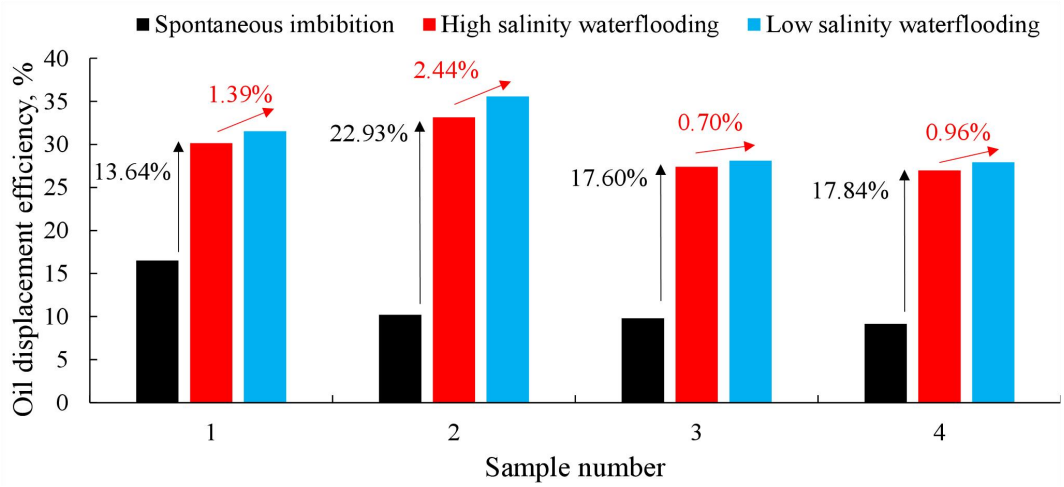


**Figure 7—Oil displacement efficiency of different stages**

**The Impact of Wettability Alteration on Waterflooding Recovery**. As **Figure 8** shows, we used rock cores to measure the wettability, and the results showed that the contact angle gradually increased from No. 1 to No. 4 samples, indicating that the degree of hydrophilic became weaker. However, due to the pore boundary angle condition, as shown in Figure 7, the waterflooding efficiency of the No. 1 sample is the lowest. That is, too strong hydrophilic will lead to too much residual oil due to corner flow.

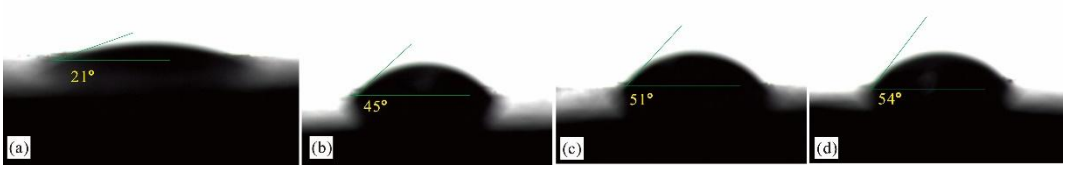


**Figure 8—Contact angle measurement for (a) Sample 1, (b) Sample 2, (c) Sample 3, and (d) Sample 4.**

By extracting the oil phase in the pore space, we found that the residual oil in sample 1 was indeed more than that in other samples (**Figure 9**), which showed that strong water film displacement would lead to a fast penetration rate, resulting in too much residual oil in the form of dots, affecting the waterflooding recovery.

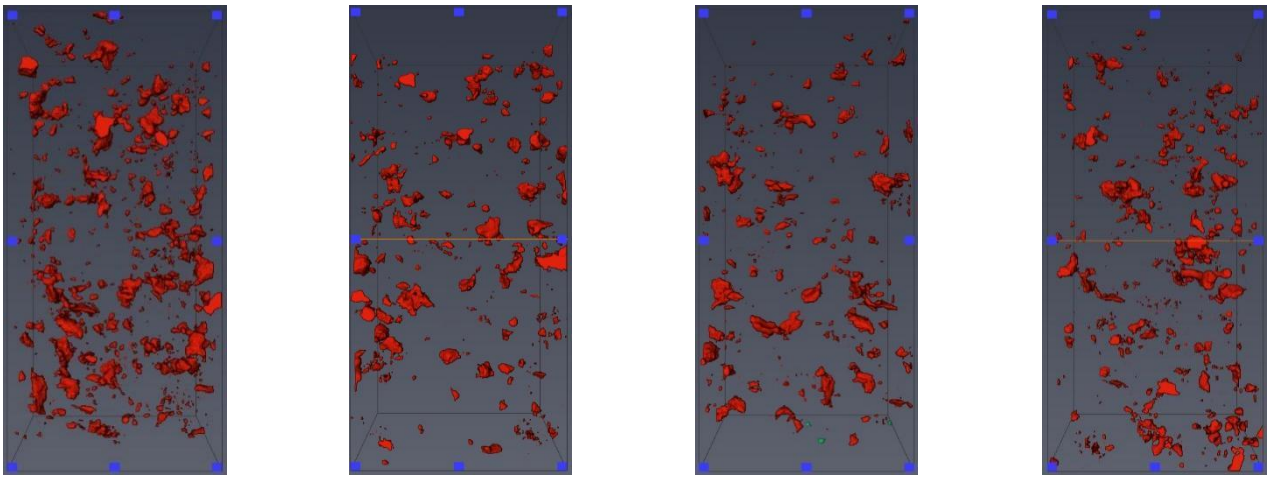

(a) Sample 1 (b) Sample 2 (c) Sample 3 (d) Sample 4

**Figure 9—Residual oil distributions for different samples**

**Effect of Pore Structures on Oil Displacement Efficiency.** Using the combined method of nuclear magnetic resonance and high-pressure mercury injection, the factors affecting the pore structure of the mainstream zone of water-flooding are explored. In this study, we compared the samples after oil saturation and waterflooding with low salinity to obtain a waterflooding space. The space that accounts for 80 % of the waterflooding space is defined as the mainstream waterflooding zone, which is coupled with the pore size distribution to calculate the average pore size of the mainstream waterflooding space. As shown in **Figure 10**, sample 2 has the largest dis-placement zone, which means the highest oil displacement efficiency. Sample 1 has the largest average pore size in the mainstream displacement zone, sample 3 is in the middle, and sample 4 has almost no displacement zone. This result corresponds to the previous research results, indicating that pore size is not a decisive factor in determining water-flooding efficiency. Excessive water wettability can easily lead to leading edge protrusion, and even large pore sizes cannot offset the dotted residual oil distribution caused by corner flow.

## Conclusions

Capillary imbibition and viscous displacement are the main driving forces during waterflooding, and understanding them can help to formulate waterflooding plans. In this study, CT and other means were used to carry out spontaneous imbibition and salinity waterflooding experiments, and the following conclusions were obtained:

1. Spontaneous imbibition has little impact on oil displacement efficiency. Water flooding can significantly improve oil displacement efficiency, but due to pressure drop constraints, its spread is severely limited. Low salinity water can further improve oil recovery.
2. Changes in wettability are the key microscopic mechanism for improving oil dis-placement efficiency, corner flow seriously affects displacement efficiency.
3. The excessive hydrophilic condition can lead to severe corner flow. Under this premise, the pore size cannot directly control the displacement efficiency. Severe corner flow can cause leading edge protrusion, leading to the widespread distribution of drop-shaped residual oil, seriously restricting the improvement of displacement efficiency in the later stage.

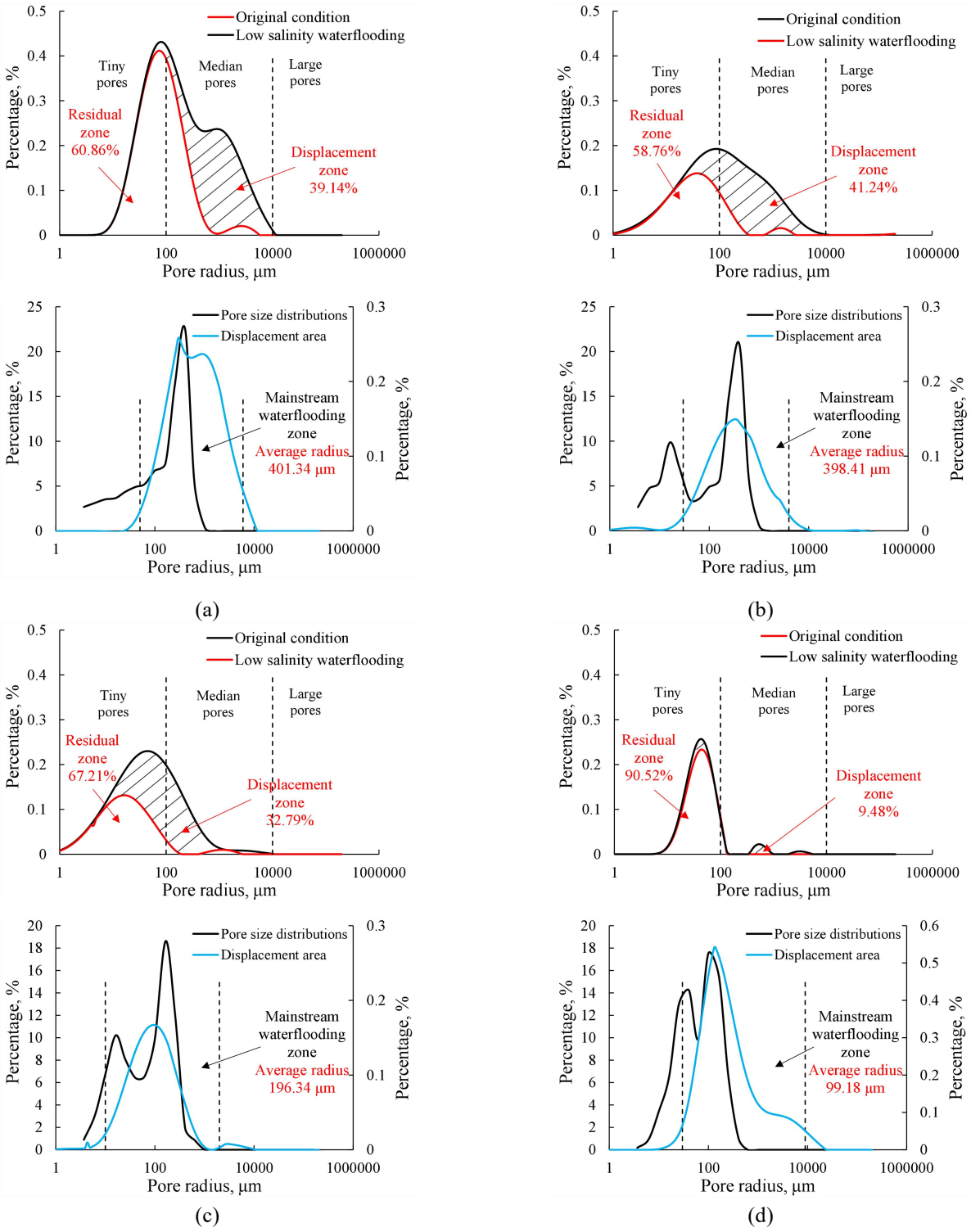


**Figure 10—Pore size and waterflooding zone combined with nuclear magnetic resonance and high-pressure mercury injection.**

## References


Aksu, I., Bazilevskaya, E., and Karpyn, Z. 2015. Swelling of Clay Minerals in Unconsolidated Porous Media and Its Impact on Permeability. *GeoResJ* **7**:1-13.

Amirian, T., Haghighi, M., Sun, C., et al. 2019. Geochemical Modeling and Microfluidic Experiments to Analyze Impact of Clay Type and Cations on Low-Salinity Water Flooding. *Energy & Fuels* **33**(4): 2888-2896.

Awolayo, A., Sarma, H., AlSumaiti, A. 2016. An Experimental Investigation into the Impact of Sulfate Ions in Smart Water to Improve Oil Recovery in Carbonate Reservoirs. *Transport in Porous Media* **111**: 649-668.

Dordzie, G. and Dejam, M. 2021. Enhanced Oil Recovery from Fractured Carbonate Reservoirs Using Nanoparticles with Low Salinity Water and Surfactant: A Review on Experimental and Simulation Studies. *Advances in Colloid and Interface Science* **293**:102449.

Druetta, P., Raffa, P., Picchioni, F. 2019. Chemical Enhanced Oil Recovery and the Role of Chemical Product Design. *Applied Energy* **252**:113480.

Fani, M., Pourafshary, P., Mostaghimi, P., et al. 2022. Application of Microfluidics in Chemical Enhanced Oil Recovery: A Review. *Fuel* **315**:123225.

Kamal, M.S., Mahmoud, M., Hanfi, M., et al. 2019. Clay Minerals Damage Quantification in Sandstone Rocks Using Core Flooding and NMR. *Journal of Petroleum Exploration and Production Technology* **9**:593-603.

Kooli, F., Yan, L., Tan, S., et al. 2014. Organoclays from Alkaline-treated Acid-activated Clays: Properties and Thermal Stability. *Journal of Thermal Analysis and Calorimetry* **115**:1465-75.

Krumbein, W.C. 1941. Measurement and Geological Significance of Shape and Roundness of Sedimentary Particles. *Journal of Sedimentary Research* **11**(2):64-72.

Lebedev, M., Zhang, Y., Sarmadivaleh, M., et al. 2017. Carbon Geosequestration in Limestone: Pore-Scale Dissolution and Geomechanical Weakening. *International Journal of Greenhouse Gas Control* **66**:106-19.

Liu, Z., Yang, Y., Yao, J., et al. 2017. Pore-scale Remaining Oil Distribution Under Different Pore Volume Water Injection Based on CT Technology. *Advances in Geo-Energy Research* **1**(3):171-181.

Mayo, S., Josh, M., Nesterets, Y., et al. 2015. Quantitative Micro-Porosity Characterization Using Synchrotron Micro-CT and Xenon K-Edge Subtraction in Sandstones, Carbonates, Shales and Coal. *Fuel* **154**:167-73.

Rücker, M., Berg, S., Armstrong, R., et al. 2015. From Connected Pathway Flow to Ganglion Dynamics. *Geophysical Research Letters* **42**(10):3888-3894.

Sameni, A., Pourafshary, P., Ghanbarzadeh, M., et al. 2015. Effect of Nanoparticles on Clay Swelling and Migration. *Egyptian Journal of Petroleum* **24**(4):429-437.

Song, W. and Kovscek, A.R. 2015. Functionalization of Micromodels with Kaolinite for Investigation of Low Salinity Oil-recovery Processes. *Lab on a Chip* **15**(16):3314-25.

Sun, X., Zhang, Y., Chen, G., et al. 2017. Application of Nanoparticles in Enhanced Oil Recovery: a Critical Review of Recent Progress. *Energies* **10**(3):345-352.

Watson, R.D. and Weinstein, L.M. 1971. A Study of Hypersonic Corner Flow Interactions. *AIAA Journal* **9**(7):1280-1286.

Xu, D., Bai, B., Wu, H., et al. 2019. Mechanisms of Imbibition Enhanced Oil Recovery in Low Permeability Reservoirs: Effect of IFT Reduction and Wettability Alteration. *Fuel* **244**:110-119.

**Cheng Liu** is a senior engineer in CNOOC EnerTech-Drilling & Production Co. His research interests include unconventional oil and gas reservoir core analysis experiment and seepage experiment. Liu holds a master's degree in engineering from China University of Mining and Technology.

**Yanjun Yin** is a Senior Reservoir Engineer in CNOOC. His research interests include reservoir development plan, reservoir simulation. Yin holds a bachelor's degree from Northeast Petroleum University, China, a master's degree from China University of Petroleum, Beijing.

**Ruiting Bao** is a Reservoir Engineer in CNOOC. Her research interests include unconventional resources， Comprehensive treatment of old oil fields. Bai holds a master's degree in petroleum engineering from Xi'an Shiyou University and a PhD degree in petroleum engineering from China University of Geosciences, Beijing.

**Dengke Liu** is a Associate Professor in the School of Human Settlements and Civil Engineering at Xi'an Jiaotong University. His research interests include unconventional resources' pore structures and fluid flow behavior. Liu holds a bachelor's degree in geology from Northwest University, China, and a PhD degree in mineral prospecting and exploration from Northwest University, China and University of Alberta.